PRAMANA — journal of physics

Vol. 83, No. 6
December 2014
pp. 975–983

Shape of Te isotopes in mean-field formalism

T BAYRAM[1,*] and A H YILMAZ[2]

[1]Department of Physics, Sinop University, 57000 Sinop, Turkey
[2]Department of Physics, Karadeniz Technical University, 61080 Trabzon, Turkey
*Corresponding author. E-mail: tbayram@sinop.edu.tr

MS received 8 February 2013; revised 14 February 2014; accepted 4 March 2014
DOI: 10.1007/s12043-014-0816-4; ***e*Publication:** 22 November 2014

Abstract. The systematic investigation of ground-state shape evolution from γ-unstable $O(6)$ to spherical $U(5)$ for even−even $^{112-134}$Te has been presented by using the quadrupole moment-constrained Hartree–Fock–Bogoliubov (HFB) method. By examining potential energy curves of Te isotopes, it has been suggested that ^{124}Te nucleus may hold $E(5)$ symmetry.

Keywords. Hartree–Fock–Bogoliubov method; shape evolution; quantum phase transition; potential energy curves.

PACS Nos 21.10.Dr; 21.10.Ky; 21.60.Jz

1. Introduction

Spherical vibrator, rotational ellipsoid, and other deformed shapes are intimately linked to the various modes of collective motion [1–3]. Depending on the changes in proton and neutron numbers, nuclei can alter their energy levels and electromagnetic transition rates among their collective modes. These changes from one kind of collective behaviour to another are known as shape phase transition. These transitions are quantum phase transitions (QPTs) [4]. However, QPTs are different from thermal phase transitions which are functions of temperature. QPT implies changes in the shape of the nucleus and the control parameter is the nucleon number. In the last decade, many researchers have given insights into structural evolution of nuclei (in particular, transitional regions of rapid change) [5]. They have used the concepts of QPTs, phase coexistence, critical-point symmetries [6,7], as well as geometrical models [8–13].

Theoretically, QPTs have been mostly studied within the interacting boson model (IBM). It holds the $U(5)$, $SU(3)$ and $O(6)$ symmetries within the simplest $U(6)$ symmetry. The $U(5)$, $SU(3)$ and $O(6)$ dynamical symmetries correspond to the shape phase of a spheroid, axially prolate rotor and γ-soft rotor, respectively [14]. Using the model, Ginocchio and Kirson [15] and Dieperink *et al* [16] have pointed out that first-order transition occurs between $O(6)$ and $SU(3)$ and second-order transition take places between

$U(5)$ and $O(6)$. More recently, Iachello has shown that special solutions of Bohr Hamiltonian can describe the properties of nuclei lying at the critical-point symmetries $E(5)$ and $X(5)$ which correspond to the second-order [6] and first-order transitions [7], respectively. Experimentally, the $E(5)$ and $X(5)$ symmetries have been realized in the spectrum of ^{134}Ba [17] and ^{152}Sm [18], respectively. These experimental realizations have triggered many works on quantum phase transitions.

In the recent decade, mean-field formalisms (e.g., HFB method [19–21] and relativistic mean field (RMF) model [22–25]) which predict many nuclear phenomena, have been successfully employed to investigate shape phase transition in nuclei. The RMF theory has been used to investigate the critical-point nuclei in even–even Sm [26] and Ce [27] isotopes. In these studies, ^{148,150,152}Sm and ^{128,130,132,134}Ce have been suggested as examples of the possible nuclei with $X(5)$ symmetry. Besides, Ti isotopes have been examined in the HFB method [28] and RMF model [29] to investigate the critical-point nuclei. In these studies, ^{48,52,60}Ti and ^{46,52,60}Ti have been found to be critical-point nuclei with $E(5)$ symmetry. Many isotopic chains in the rare-earth region have been found to be critical-point nuclei [30,31]. Also, Mo isotopes were investigated by using the RMF theory [32,33] and Yao and Guo [32] suggested ^{94}Mo to be a γ-unstable nucleus. In these studies, potential energy curves (PECs) obtained from constrained calculations have been examined to identify the critical-point nuclei. For $E(5)$ and $X(5)$ symmetries, relatively flat PECs and PECs with a bump are obtained, respectively (the relation between shape phase transition and PECs can be found in [5,34]). However, for a quantitative analysis, electromagnetic transition rates and ratios of excitation energies of nuclei should be calculated [35]. For this reason, the generator coordinate method (GCM) has been used to employ configuration mixing of angular momentum and particle-number projected relativistic wave functions [36]. In recent years, the GCM has been extended on triaxial states [37–39]. However, the application of these methods in a systematic study of shape transition is still very time-consuming at present because of its triaxiality. It should be noted, however, that the PECs obtained from constrained calculations are important, and can provide a qualitative understanding of the QPT. Particularly, the evolution of PECs along the isotopic or isotonic chains can be useful for investigating shape phase transitions in nuclei.

Rapid structural evolution in nuclei has been known for about half a century [5]. Classic shape transition regions occur in the light Si–Mg region [40], near $A = 100$ ($Z \sim 40$) [41], light rare-earth region ($A \sim 150$) and actinide region. Besides, the γ-unstable character of nuclei in the mass region $A = 120$–130 was investigated many years ago [42]. ^{124}Te in this region was experimentally investigated and suggested to be a possible γ-soft nucleus [43]. In the present study, constrained HFB method has been employed to obtain the ground-state properties of $^{112-134}$Te isotopes, such as total binding energy and quadrupole deformation. The shape evolution of Te isotopes has been analysed by examining their PECs.

2. Details of calculations

In the present study, the program HFBTHO (v1.66p) [44] is used to carry out ground-state properties of even−even Te isotopes within the framework of HFB

method. In this method, a two-body Hamiltonian of a system of fermions is given by

$$H = \sum_{n_1 n_2} e_{n_1 n_2} c^{\dagger}_{n_1} c_{n_2} + \frac{1}{4} \sum_{n_1 n_2 n_3 n_4} \bar{\upsilon}_{n_1 n_2 n_3 n_4} c^{\dagger}_{n_1} c^{\dagger}_{n_2} c_{n_4} c_{n_3} \,, \tag{1}$$

where $\bar{\upsilon}_{n_1 n_2 n_3 n_4} = \langle n_1 n_2 | V | n_3 n_4 - n_4 n_3 \rangle$ are antisymmetrized matrix elements of N–N interaction and c ($c^{\dagger}$) is the annihilation (creation) operator. The ground-state wave function $|\Phi\rangle$ is described as the quasiparticle vacuum $\alpha_k |\Phi\rangle = 0$ and the linear Bogoliubov transformation

$$\alpha_k = \sum_n (U^*_{nk} c_n + V^*_{nk} c^{\dagger}_n), \quad \alpha^{\dagger}_k = \sum_n (V_{nk} c_n + U_{nk} c^{\dagger}_n) \tag{2}$$

provides connection between the quasiparticle operators ($\alpha, \alpha^{\dagger}$) and the original particle operators. The method is mainly based on the density matrix and the pairing tensor. In terms of the normal ρ and pairing κ one-body density matrices are given by

$$\rho_{nn'} = \langle \Phi | c^{\dagger}_{n'} c_n | \Phi \rangle = (V^* V^T)_{nn'}, \quad \kappa_{nn'} = \langle \Phi | c_{n'} c_n | \Phi \rangle = (V^* U^T)_{nn'} \,. \tag{3}$$

The expectation value of the Hamiltonian (1) can be expressed in terms of an energy functional:

$$E[\rho, \kappa] = \frac{\langle \Phi | H | \Phi \rangle}{\langle \Phi | \Phi \rangle} = \mathrm{Tr}\left[\left(e + \frac{1}{2} \Gamma \right) \rho \right] - \frac{1}{2} \mathrm{Tr}[\Delta \kappa^*], \tag{4}$$

where $\Gamma_{n_1 n_3} = \sum_{n_2 n 4} \bar{\upsilon}_{n_1 n_2 n_3 n_4} \rho_{n_4 n_2}$ and $\Delta_{n_1 n_2} = \frac{1}{2} \sum_{n_3 n 4} \bar{\upsilon}_{n_1 n_2 n_3 n_4} \kappa_{n_3 n_4}$. By means of the Skyrme forces, the HFB energy (4) has the form of local energy density functional:

$$E[\rho, \tilde{\rho}] = \int \mathrm{d}^3 \mathrm{H}(\mathbf{r}), \tag{5}$$

where $\mathrm{H}(\mathbf{r}) = H(\mathbf{r}) + \tilde{H}(\mathbf{r})$ is the sum of the mean-field and pairing energy densities. The variation of the energy (5) in terms of ρ and $\tilde{\rho}$ results in Skyrme HFB equations:

$$\sum_{\sigma'} \begin{pmatrix} h(\mathbf{r}, \sigma, \sigma') & \tilde{h}(\mathbf{r}, \sigma, \sigma') \\ \tilde{h}(\mathbf{r}, \sigma, \sigma') & -h(\mathbf{r}, \sigma, \sigma') \end{pmatrix} \begin{pmatrix} U(E, \mathbf{r}\sigma') \\ V(E, \mathbf{r}\sigma') \end{pmatrix} = \begin{pmatrix} E + \lambda & 0 \\ 0 & E - \lambda) \end{pmatrix} \begin{pmatrix} U(E, \mathbf{r}\sigma) \\ V(E, \mathbf{r}\sigma) \end{pmatrix}, \tag{6}$$

where λ is the chemical potential. $h(\mathbf{r}, \sigma, \sigma')$ and $\tilde{h}(\mathbf{r}, \sigma, \sigma')$ can be obtained in the coordinate space [19,44].

The HFB equations (5) can be solved by expanding quasiparticle wave functions that conserve parity and axial symmetry on a harmonic oscillator basis expressed in coordinate space as proposed in ref. [44]. For pairing, the zero-range pairing interaction has been considered and Lipkin–Nogami method has been employed. The oscillator parameter b_0 has been taken as

$$b_0 = \sqrt{2(\hbar^2/2m)(49.2A^{-1/3})}. \tag{7}$$

To obtain the PECs in the present study, the standard quadratic form of the quadrupole constraint [20,44] has been performed. Sixteen oscillator shells have been taken into account in the present calculations. A number of effective Skyrme forces can be found in [45–47]. In this work, the widely used Skyrme force SLy4 [47] has been employed to calculate properties of even−even Te isotopes with $60 \leq N \leq 82$.

3. Results and discussions

The calculated ground-state binding energies for even−even $^{112-134}$Te isotopes obtained from the constrained HFB method are tabulated in table 1. Also, the predictions of RMF model [48] and the experimental data [49] are listed. The total binding energies of all isotopes are reproduced well by the SLy4 Skyrme force. The deviations are at most 0.3%. Also, as can be seen in table 1, the predictions of RMF model with NL3 interaction are in a good agreement with the available experimental results. The mean differences between experimental data and the predictions of the HFB method and RMF model with NL3 interaction are 2.532 and 1.688 MeV, respectively. For this reason, it can be pointed out that the predictions of both HFB method and RMF model are good in describing the ground-state binding energies of $^{112-134}$Te.

The mean-field formalism based on the Hartree–Fock approximation with phenomenological effective interactions is important in the microscopic description of nuclei [50,51]. It allows a unified description for properties of nuclei throughout the nuclidic chart. One of the great achievements of the theory is that it not only reproduces binding energies and densities, but also provides a good description of the ground-state deformations in nuclei [52]. In this study, the quadrupole deformation parameters β_2 for $^{112-134}$Te have been obtained from constrained HFB method with SLy4 Skyrme force. They are shown in figure 1. Also, the predictions of RMF model [48] and the experimental data [53] are shown. The calculated β_2 values obtained from HFB method with SLy4 parameters are found to be in good agreement with the experimental data. Only the amplitude of quadrupole deformation parameter β_2 obtained from HFB method and RMF model are given in figure 1. The exact values of β_2 are listed in table 2. It should be noted, however, that β_2 cannot be observed directly in an experiment. To obtain experimental β_2, a conventional way is to use electric quadrupole transition rate from the ground-state 0^+ to the 2^+ state $B(E2)\uparrow$ [53]. The correlation between $B(E2)\uparrow$ and β_2 can be given by the formula $\beta_2 = (4\pi/3ZR_0^2)[B(E2)\uparrow/e^2]^{1/2}$ where $R_0 = 1.2A^{1/3}$. The formula based on rigid rotor cannot always represent a parameter of deformation. Extracting β_2 is

Table 1. The total binding energies for the ground-state of $^{112-134}$Te in units of MeV.

Te isotopes	This work	RMF [48]	Exp. [49]
^{112}Te	937.821	938.880	940.610
^{114}Te	958.058	959.060	961.337
^{116}Te	977.630	978.530	980.860
^{118}Te	996.680	997.600	999.454
^{120}Te	1014.148	1015.640	1017.281
^{122}Te	1030.893	1032.530	1034.333
^{124}Te	1047.472	1049.160	1050.686
^{126}Te	1063.296	1066.980	1066.368
^{128}Te	1078.858	1080.750	1081.439
^{130}Te	1094.204	1096.430	1095.941
^{132}Te	1108.850	1112.220	1109.914
^{134}Te	1123.508	1126.430	1123.435

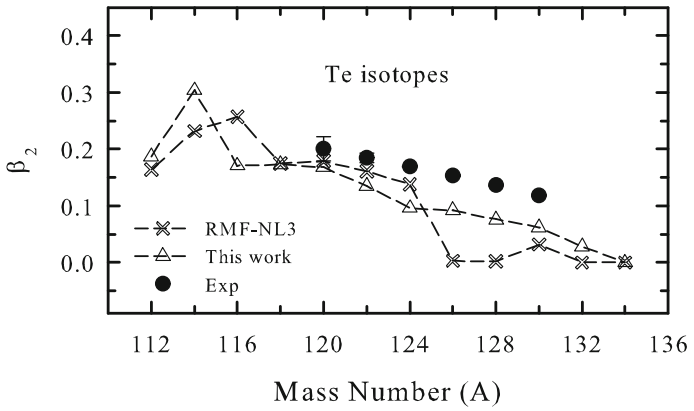

Figure 1. The ground-state quadrupole deformation parameters for Te isotopes. The predictions of the HFB method with SLy4 Skyrme force are compared with those of the RMF model with NL3 interaction [48] and experimental results [49].

questionable in the case of spherical nuclei, because $B(E2)\uparrow$ connects vibrational states in the spherical nuclei. In particular, the radius R_0 is so small for light nuclei. This elicits a very large β_2 deformation with the formula. However, this formula is suitable in medium-mass and heavy regions [29].

The $E(5)$ critical-point symmetry is related to the shape transition from spherical to γ-unstable nuclei. It has been carried out as a special case of the Bohr Hamiltonian [6]. Besides, IBM Hamiltonian at the critical point in the transition from spherical to γ-unstable shape can be represented in the geometrical model by a β^4 potential. The potential is presumed to depend only on the collective variable β and not on γ. The $E(5)$ critical-point symmetry corresponds to a flat-bottomed potential. Systematic investigations on the shape evolution of some isotopic chains involving nuclei, suggested to be

Table 2. The ground-state quadrupole deformation parameters (β_2) for Te isotopes.

Te isotopes	This work	RMF [48]	Exp. [49]
^{112}Te	0.187	0.164	
^{114}Te	0.304	0.232	
^{116}Te	−0.171	0.257	
^{118}Te	−0.173	0.175	
^{120}Te	−0.169	0.179	0.201
^{122}Te	−0.135	0.161	0.185
^{124}Te	−0.096	0.138	0.170
^{126}Te	−0.093	−0.003	0.153
^{128}Te	0.076	−0.002	0.136
^{130}Te	0.062	0.032	0.118
^{132}Te	0.028	0.000	
^{134}Te	−0.005	0.000	

possible examples of critical-point nuclei with $E(5)$ symmetry, have been carried out by using RMF model [30] and HFB method [31]. In these studies, rather flat PECs for the nuclei suggested as good examples of $E(5)$ symmetry have been found. In figure 2, we show the PECs of $^{112-134}$Te. In the figure, the total binding energy of Te isotopes for the ground state has been considered as the reference. In figure 2, starting from PEC of ^{112}Te to ^{122}Te, the nuclei have oblate shape. In the PECs of the $^{124-128}$Te, their barriers against deformation are weak which means that these nuclei may be in a transitional region. In particular, the PEC of ^{124}Te in figure 2 seems flat from $\beta_2 = -0.2$ to $\beta_2 = 0.25$. Through these β_2 ranges, the variation of the energies in the PEC of ^{124}Te are less than 0.4 MeV. This implies that the barriers against deformation are very weak, and ^{124}Te may be a possible example of the critical-point nuclei with $E(5)$ symmetry. The PEC of ^{130}Te exhibits slight preference for a prolate shape. PEC of ^{132}Te in figure 2 indicates that ^{132}Te is very close to spherical shape. Finally, ^{134}Te which has shell closure, at magic neutron number $N = 82$, is found to have a spherical shape.

In table 3, the energy differences between the spherical shape and the ground-state shape of even–even $^{112-134}$Te isotopes are given to show how the shape of the Te isotopes changes with the neutron number as an additional evidence to the results of the PECs. They can show how soft the nucleus is against deformation. The calculated binding energy differences between the spherical state and the ground state of $^{112-134}$Te isotopes change from 0 to 2.572 MeV. Binding energy differences show drastic changes in $^{120-124}$Te. A clear jump can be seen at ^{124}Te which implies that ^{124}Te can be a possible candidate for critical-point nuclei with $E(5)$ symmetry.

Some observables can be found as additional evidences for the confirmation of the result of this study. The ratios of experimental excitation energies of ^{124}Te [43] are given in table 4. The $U(5)$, $X(5)$, $SU(3)$, $E(5)$ and $O(6)$ symmetry predictions are also listed for

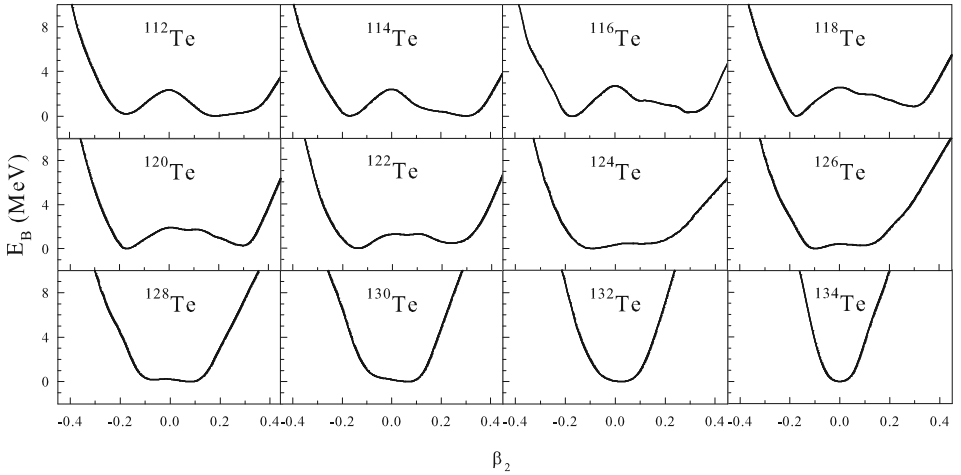

Figure 2. The potential energy curves for $^{112-134}$Te obtained from the constrained HFB method with SLy4 Skyrme force.

Table 3. The difference of the total binding energies (in units of MeV) between the spherical state and the ground state of $^{112-134}$Te obtained by the constrained HFB method with SLy4 Skyrme force.

Nuclei	HFB-SLy4
^{112}Te	2.329
^{114}Te	2.397
^{116}Te	2.519
^{118}Te	2.572
^{120}Te	1.900
^{122}Te	1.259
^{124}Te	0.354
^{126}Te	0.410
^{128}Te	0.227
^{130}Te	0.160
^{132}Te	0.053
^{134}Te	0.000

Table 4. The ratios of available experimental excitation energies for ^{124}Te isotopes compared with some theoretical predictions [5–7,43].

Symmetry	$R_{4/2}$	$R_{0/2}$
$U(5)$	2.00	2.00
$X(5)$	2.91	5.67
$SU(3)$	3.33	$\gg 2$
$E(5)$	2.20	3.03
$O(6)$	2.50	4.50
Exp.	2.07	2.75

comparison [6,7,43]. The characteristic ratio $R_{4/2} = E(4_1^+)/E(2_1^+)$ and the ratio of the energies of the first two excited 0^+ states $R_{0/2} = E(0_2^+)/E(2_1^+)$ are tabulated. As can be seen in table 4, the $E(5)$ symmetry values obtained from solution of Bohr–Mottelson differential equations for $R_{4/2}$ and $R_{0/2}$ are 2.20 and 3.03, respectively. They are closer to the observed ratios $R_{4/2} = 2.07$ and $R_{0/2} = 2.75$.

4. Summary

The values of total binding energies and quadrupole deformation parameters for even−even $^{112-134}$Te isotopes calculated in the constrained HFB method with Skyrme

SLy4 force are in a good agreement with experimental data. The ground-state shape evolution of Te isotopic chain has been investigated by using the potential energy curves. ^{124}Te has been found to be an example for possible critical-point nucleus, which marks the phase transition between spherical $U(5)$ and γ-unstable shapes $O(6)$.

References

[1] A Bohr and B R Mottelson, *Nuclear structure: Nuclear deformations* (World Scientific, Singapore, 1998)
[2] W Greiner and J A Maruhn, *Nuclear models* (Springer-Verlag, Berlin, 1996)
[3] S Ćwiok, P-H Heenen and W Nazarewicz, *Nature* **433**, 705 (2005)
[4] F Iachello, *Int. J. Mod. Phys. B* **20**, 2687 (2006)
[5] R F Casten and E A McCutchan, *J. Phys. G* **34**, R285 (2007)
[6] F Iachello, *Phys. Rev. Lett.* **85**, 3580 (2000)
[7] F Iachello, *Phys. Rev. Lett.* **87**, 052502 (2001)
[8] M A Caprio, *Phys. Rev. C* **65**, 031304 (2002)
[9] F Iachello, *Phys. Rev. Lett.* **91**, 132502 (2003)
[10] L Fortunato, *Phys. Rev. C* **70**, 011302 (2004)
[11] D Bonatsos, D Lennis, D Minkov, P P Raychev and P A Terziev, *Phys. Rev. C* **69**, 014302 (2004)
[12] F Iachello, *Phys. Rev. Lett.* **95**, 052503 (2005)
[13] D Bonatsos, D Lennis, D Petrellis, P A Terziev and I Yigitoglu, *Phys. Lett. B* **632**, 238 (2006)
[14] F Iachello and A Arima, *The interacting boson model* (Cambridge University Press, Cambridge, 1987)
[15] J N Ginocchio and M W Kirson, *Phys. Rev. Lett.* **44**, 1744 (1980)
[16] A E L Dieperink, O Scholten and F Iachello, *Phys. Rev. Lett.* **44**, 1747 (1980)
[17] R F Casten and N V Zamfir, *Phys. Rev. Lett.* **85**, 3584 (2000)
[18] R F Casten and N V Zamfir, *Phys. Rev. Lett.* **87**, 052503 (2001)
[19] P Ring and P Schuck, *The nuclear many-body problem* (Springer-Verlag, Berlin, 1980)
[20] H Flocard, P Quentin, A K Kerman and D Vautherin, *Nucl. Phys. A* **203**, 433 (1973)
[21] J Decharge and D Gogny, *Phys. Rev. C* **21**, 1568 (1980)
[22] B D Serot and J D Walecka, *Adv. Nucl. Phys.* **16**, 1 (1986)
[23] Y K Gambhir, P Ring and A Thimet, *Ann. Phys.* **198**, 132 (1990)
[24] P Ring, *Prog. Part. Nucl. Phys.* **37**, 193 (1996)
[25] J Meng, H Toki, S G Zhou, S Q Zhang, W H Long and L S Geng, *Prog. Part. Nucl. Phys.* **57**, 470 (2006)
[26] J Meng, W Zhang, S G Zhou, H Toki and L S Geng, *Eur. Phys. J. A* **25**, 23 (2005)
[27] M Yu, P-F Zhang, T-N Ruan and J-Y Guo, *Int. J. Mod. Phys. E* **15**, 939 (2006)
[28] T Bayram, *Mod. Phys. Lett. A* **27**, 1250162 (2012)
[29] J-Y Guo, X Z Fang and Z Q Sheng, *Int. J. Mod. Phys. E* **17**, 539 (2008)
[30] R Fossion, D Bonatsos and G A Lalazissis, *Phys. Rev. C* **73**, 044310 (2006)
[31] R Rodríguez-Guzmán and P Sarriguren, *Phys. Rev. C* **76**, 064303 (2007)
[32] B-M Yao and J-Y Guo, *Mod. Phys. Lett. A* **25**, 1177 (2010)
[33] A H Yilmaz and T Bayram, *J. Korean. Phys. Soc.* **59**, 3329 (2011)
[34] J M Eisenberg and W Greiner, *Nuclear theory* (North-Holland, Amsterdam, 1987) Vol. I
[35] Z P Li, T Nikšić, D Vretenar and J Meng, *Phys. Rev. C* **81**, 034316 (2010)
[36] T Nikšić, D Vretenar, G A Lalazissis and P Ring, *Phys. Rev. Lett.* **99**, 092502 (2007)

[37] M Bender and P-H Heenen, *Phys. Rev. C* **78**, 024309 (2008)
[38] J M Yao, J Meng, P Ring and D Vretenar, *Phys. Rev. C* **81**, 044311 (2010)
[39] T R. Rodríguez and J L Egido, *Phys. Rev. C* **81**, 064323 (2010)
[40] D A Bromley, H E Gove and A E Literland, *Can. J. Phys.* **35**, 1057 (1957)
[41] E Cheifetz, R C Jared, S G Thomson and J B Wilhelmy, *Phys. Rev. Lett.* **25**, 38 (1970)
[42] G Gneuss and W Greiner, *Nucl. Phys. A* **171** 449 (1971)
[43] A R H Subber, P Park, W D Hamilton, K Kumar, K Schreckenbach and G Colvin, *J. Phys. G* **12**, 881 (1986)
[44] M V Stoitsov, J Dobaczewski, W Nazarewicz and P Ring, *Comp. Phys. Commun.* **167**, 43 (2005)
[45] J Bartel, P Quentin, M Brack, C Guet and H B Hakansson, *Nucl. Phys. A* **386**, 79 (1982)
[46] A Baran, J L Egido, B Nerlo-Pomorska, K Pomorski, P Ring and L M Robledo, *J. Phys. G* **21**, 657 (1995)
[47] E Chabanat, P Bonche, P Haensel, J Meyer and R Schaeffer, *Nucl. Phys. A* **635**, 231 (1998)
[48] G A Lalazissis, S Raman and P Ring, *At. Data Nucl. Data Tables* **71**, 1 (1999)
[49] G Audi, A H Wapstra and C Thibault, *Nucl. Phys. A* **729**, 337 (2003)
[50] D Vautherin and D M Brink, *Phys. Rev. C* **5**, 626 (1972)
[51] D Gogny, *Nucl. Phys. A* **237**, 399 (1975)
[52] D Vautherin, *Phys. Rev. C* **7**, 296 (1973)
[53] S Raman, C W Nestor Jr and P Tikkanen, *At. Data Nucl. Data Tables* **78**, 1 (2001)